

NASA TECHNICAL NOTE



NASA TN D-5154

e.1

LOAN COPY: RETURN TO
AFWL (WLIL-2)
KIRTLAND AFB, N MEX

0131956



TECH LIBRARY KAFB, NM

NASA TN D-5154

EFFECTS OF TEMPERATURE AND ELECTROLYTE CONCENTRATION ON PERFORMANCE OF A FUEL CELL OF THE BACON TYPE

by Robert E. Post

*Lewis Research Center
Cleveland, Ohio*



EFFECTS OF TEMPERATURE AND ELECTROLYTE CONCENTRATION
ON PERFORMANCE OF A FUEL CELL OF THE BACON TYPE

By Robert E. Post
Lewis Research Center
Cleveland, Ohio

NATIONAL AERONAUTICS AND SPACE ADMINISTRATION

For sale by the Clearinghouse for Federal Scientific and Technical Information
Springfield, Virginia 22151 - CFSTI price \$3.00

ABSTRACT

Performance was studied in terms of voltage-current data for temperatures ranging from 300⁰ to 460⁰ F (422 to 511 K), KOH concentrations ranging from 70 to 82 wt. %, and reactant pressures of 22.4 psia (1.54×10^5 N/m²). The effect of increased concentration appeared as an upward displacement of the voltage-current curve and was two or more times that calculated from thermodynamic considerations. The effect of temperature appeared to be consistent with rate-process principles, in that it increased with current and decreased as equilibrium conditions were approached.

EFFECTS OF TEMPERATURE AND ELECTROLYTE CONCENTRATION ON PERFORMANCE OF A FUEL CELL OF THE BACON TYPE

by Robert E. Post
Lewis Research Center

SUMMARY

An empirical study was conducted on a cell without a reference electrode to determine the effects of temperature and aqueous potassium hydroxide (KOH) electrolyte concentration on cell performance. Performance was studied in terms of voltage-current data for temperatures ranging from 300° to 460° F (422 to 511 K) and concentrations ranging from 70 to 82 weight percent of KOH. Reactant pressure was 22.4 psia (1.54×10^5 N/m² abs). The experimental design consisted of variations of temperature and concentration about mean values. Four sets of mean values of both variables were established on the basis of minimal variation of electrolyte vapor pressure. Since concurrent increases of temperature and concentration were required in order to maintain uniform vapor pressure, and this resulted in increased performance, the concept of performance level was introduced as a parameter.

The effects of temperature T and concentration W on voltage V are represented as coefficients, designated $(\partial V / \partial T)_W$ and $(\partial V / \partial W)_T$, which were determined at three levels of current density for each performance level. Coefficients were not determined for zero current density because the open-circuit voltages exhibited a strong time dependence. These coefficients and their standard errors were estimated by regression analysis. Values of $(\partial V / \partial T)_W$ ranged from 0.9 to 23 volts per °F (1.6 to 42 V/K), increasing with current density and decreasing with performance level. Values of $(\partial V / \partial W)_T$ were considered constant at 1.0 volt per percent, within experimental error, for all conditions of current density and performance level. This value is two or more times that calculated according to thermodynamic principles.

With the use of statistical significance tests at a liberal level of 20 percent chance occurrence, the behavior of the coefficients was found to be consistent with rate-process considerations and data from other sources, except for the behavior of the concentration coefficient with respect to performance level. The variation of $(\partial V / \partial W)_T$ between performance levels has only borderline significance and, if anything, increases with performance level, which is not to be anticipated if kinetic considerations are applied. In the light of this behavior and the results of other work, it is concluded that the oxygen electrode is characterized generally by a fixed or current-independent loss and that the effect of concentration is associated with an unresolved mechanism that is responsible for this loss.

INTRODUCTION

The selection of the hydrogen-oxygen fuel cell to supply auxiliary power for intermediate-duration space missions was based on the lowest practical overall system weight which resulted from the efficient use of high-energy-density reactants. The fuel cell subcontractor for the NASA Apollo mission, Pratt & Whitney Aircraft Division of United Aircraft Corporation (P&WA), adopted a modification of a fuel cell developed by Bacon (ref. 1, ch. 5 and ref. 2, ch. 3) as the basic unit in their system. The distinguishing feature of the Bacon cell is that it is designed for operation at temperatures sufficiently high that the need for noble-metal catalysts is avoided. The electrodes are made of porous nickel sinter. Whatever catalytic activity exists resides in metallic nickel at the anode and in semiconductive nickel oxide at the cathode.

The electrolyte employed is aqueous KOH. At typical Bacon cell operating temperatures, one cannot have an electrolyte composition that is liquid at room temperature without having to deal with a rather high vapor pressure of water at the operating temperature (ref. 3). Bacon preferred low-concentration - high-vapor pressure conditions (ref. 1, ch. 5 and ref. 2, ch. 4) and compensated for high vapor pressure by employing a high operating pressure. The subcontractor chose to work with higher electrolyte concentration in spite of the necessity for preheating the cell to liquefy the electrolyte before startup (ref. 4). A comparison of conditions is shown in table I.

TABLE I. - COMPARISON OF OPERATING CONDITIONS FOR BACON
CELL WITH THOSE FOR MODIFIED BACON CELL

	Bacon cell ^a	Modified cell ^b
Temperature, T, °F; K	392; 473	500; 533
Potassium hydroxide concentration, W, wt. %	37	85
Reactant pressure, psia; N/m ² abs	400; 27.5×10 ⁵	20; 1.4×10 ⁵
Estimated vapor pressure, psia; N/m ² abs	^c 120; 8.2×10 ⁵	^d 2.45; 1.7×10 ⁵

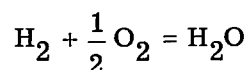
^aRef. 1.

^bRef. 4.

^cRef. 12.

^dUnpublished data obtained from Pratt & Whitney Aircraft Division of
United Aircraft Corporation

Voltage-current density data, as reported by Bacon (ref. 1, p. 62) and as determined in this laboratory (unpublished data obtained by J. McKee and N. Hagedorn of Lewis) for typical Apollo prototype test cells at slightly different conditions from those of table I, are shown in figure 1 as "Bacon (1)" and "Test cells," respectively. This figure makes evident the fact that the theoretical open-circuit voltage for the reaction



(see appendix A) is approached much more closely by the test cell curve and that superior performance is indicated up to and beyond current densities of 200 amperes per square foot (2150 A/m^2).

The fact that at higher current densities the test cell voltage falls more rapidly than that for Bacon's data is expected because of the lower pressure and higher concentration. Any process involving the diffusion or the reaction kinetics of gaseous reactants should be promoted by high pressure. As to concentration, electrolyte conductance falls with

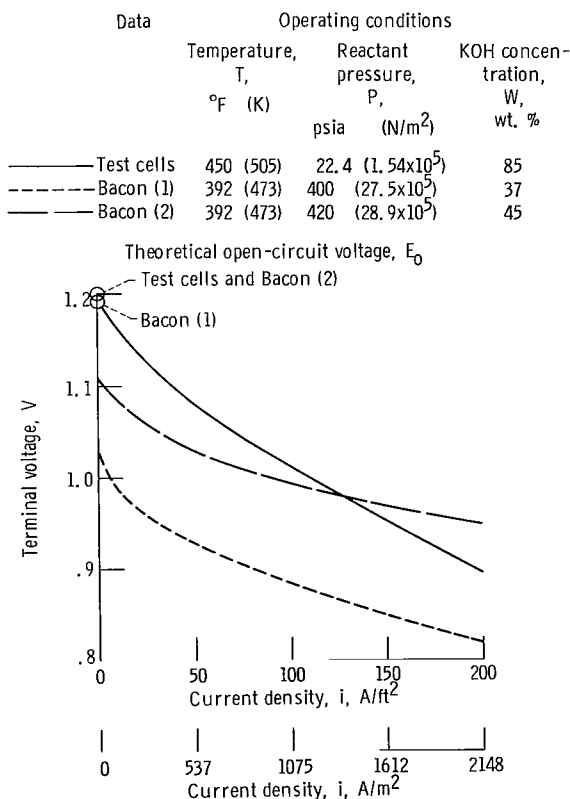


Figure 1. - Comparison of performances of Bacon cells and test cells.

increasing concentration between 37 and 85 weight percent (ref. 2), which would increase the internal resistance.

At lower current densities, if adverse effects occur from lower pressure and higher concentration, they are evidently overshadowed by some unknown factor. This factor apparently reduces a fixed loss that prevents attainment of the theoretical voltage, even at open circuit.

The source of these differences in performance characteristics might lie in the somewhat higher temperatures employed with test cells, in the higher KOH concentration, or in some property of the electrodes themselves. Since temperature and concentration are readily varied, it was decided to examine their effect on fuel cell performance using available hardware and employing an essentially empirical approach.

Later data reported by Bacon (ref. 3, p. 176) and taken at a somewhat higher KOH concentration of 45 percent support a hypothesis that concentration has an intrinsic importance. These data are plotted as Bacon (2) in figure 1. However there are also present factors of improved electrode construction and a slightly higher reactant pressure of 420 psia ($28.9 \times 10^5 \text{ N/m}^2$ abs).

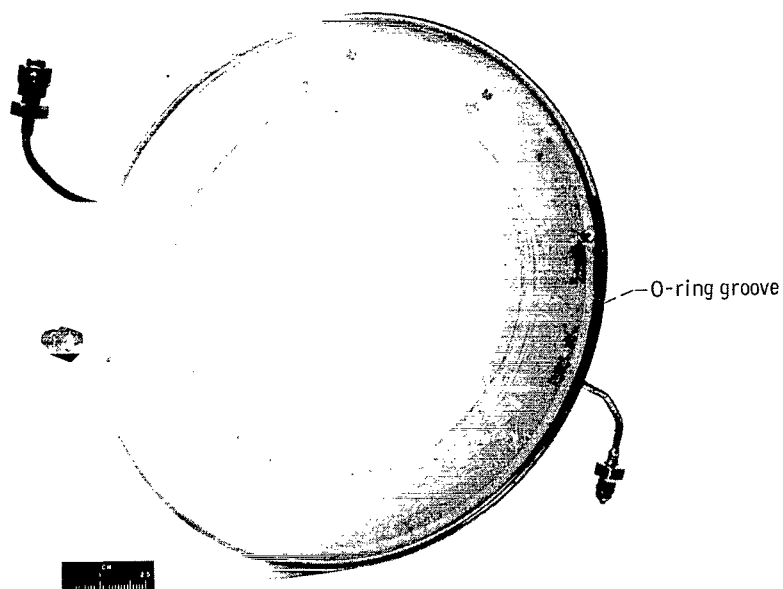
For the present investigation, the KOH concentration was varied from 70 to 82 weight percent and the temperature from 300° to 460° F (422 to 511 K). All data were obtained on the same cell with the pressure held constant at 22.4 psia ($1.54 \times 10^5 \text{ N/m}^2$ abs).

APPARATUS AND PROCEDURE

The fuel cells were prototype Apollo hardware available from a system evaluation program. The electrode construction is shown in figure 2. The porous nickel electrode is 5 inches (0.127 m) in diameter (fig. 2(a)). (The projected geometrical area is 0.136 ft^2 ($1.26 \times 10^{-2} \text{ m}^2$).) Gas passages are formed between the support plate and the electrode (fig. 2(b)). Two similar electrodes are clamped together to form a single cell. A polytetrafluoroethylene O-ring, held in grooves near the edges of the support plates, seals the electrolyte and provides electrical insulation.

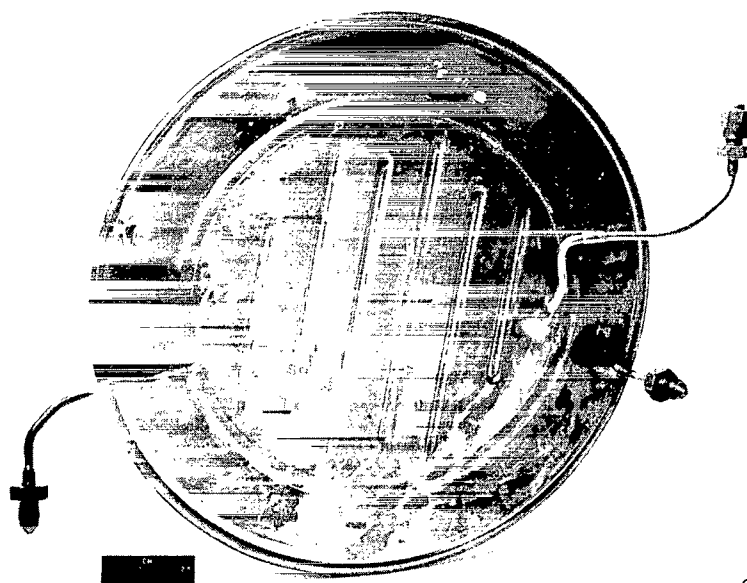
A cross section of the electrode construction is shown schematically in figure 2(c). This construction uses capillary forces to maintain the electrolyte-gas interface within the electrode. A differential pressure is applied that is greater than the bubble pressure of the coarse-pore layer but less than that of the fine-pore layer.

The electrochemical process at the oxygen electrode is generally believed to involve a wetted film extending from the meniscus toward the gas side and along the walls of the coarse-pore layer (ref. 5). Performance is sensitive to the geometry of this interface. A temporary application of a differential pressure across the oxygen electrode, some-



C-67-4118

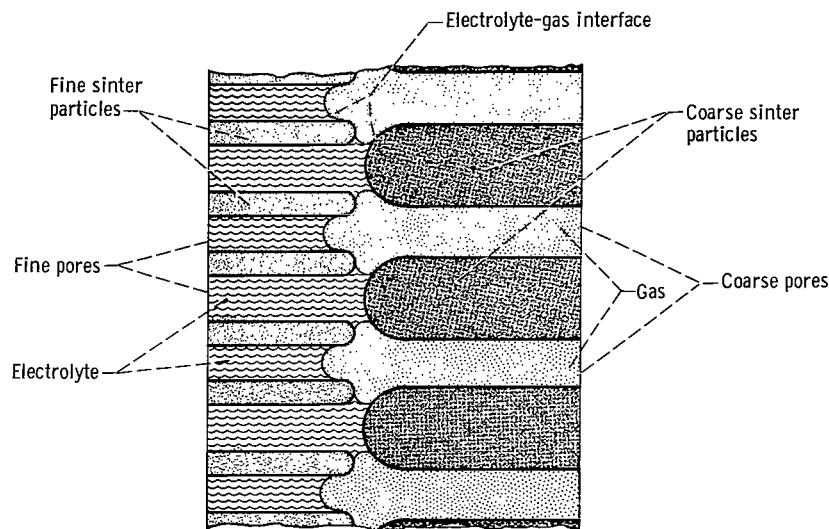
(a) Electrode and diaphragm area.



C-67-4117

(b) View of backup plate showing outlines of gas passages.

Figure 2. - Electrode assembly.



(c) Cross-sectional view of dual-porosity electrode.

Figure 2. - Concluded.

what higher than the operating pressure differential but not so high as to exceed the bubble pressure of the fine-pore layer, has been found to be effective in promoting uniform performance. This procedure was applied each day after the cell was filled and preliminary to taking the data. The operating pressure differential was 8.0 psi (0.55×10^5 N/m²). The temporary differential pressure was 9.0 psi (0.62×10^5 N/m²). The total operating pressure of the reactants was 22.4 psia (1.54×10^5 N/m²).

A view of a cell in its holder as arranged inside an oven is shown in figure 3. The outside of the hydrogen electrode is visible inside the upper clamp ring. The four tabs connected to black wires are voltage taps. Affixed to the exterior of the electrode are three thermocouple probes connected to white wires. The four heavy, stranded, uninsulated cables are current leads. The current path is radial from the electrodes through the diaphragm region and into the clamp ring from which it passes to the two cables diametrically attached to each ring.

The fuel cell voltage was read to ± 0.001 volt on a high-impedance digital voltmeter using the taps in the center of the electrodes. (Voltages at the taps nearest the current take-off connection were about 0.001 V less per each 10-A load.) The current was also read from a digital voltmeter to ± 0.1 ampere using a 0.001-ohm shunt. Temperatures were continuously recorded on a multipoint recorder using an ice bath (32° F or 273 K) reference junction. Pressures were read to ± 0.1 psig (69 N/m² gage) with precision bourdon tube gages. Pressure taps were located in the vent lines.

The cell was filled in an inclined position through the nearer of the two fill cups. A 1/8-inch (~ 3.2 -mm) tube connected the cup to the lowest point on the cell. Another

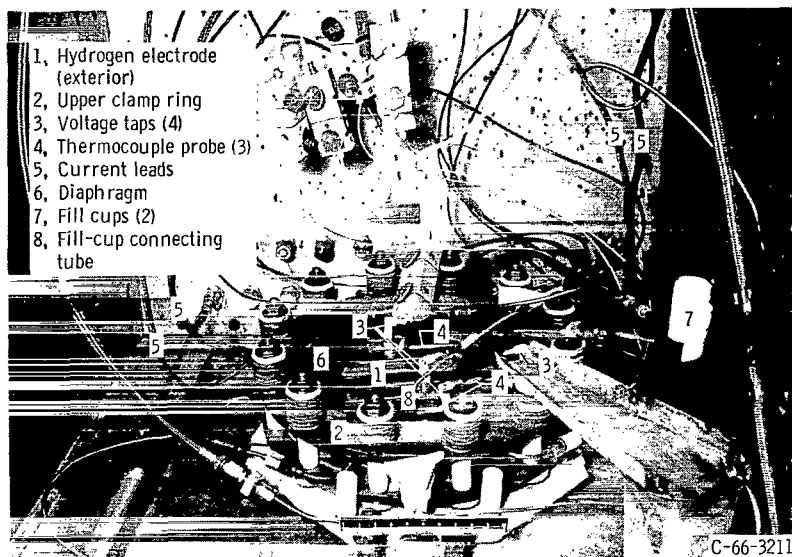


Figure 3. - Fuel cell test rig.

cup served as an overflow reservoir and was accordingly connected to the highest point. The cups held enough electrolyte to compensate for the volume change corresponding to somewhat more than a 50⁰ F (28 K) temperature change. For taking samples of the electrolyte, the cups were removed, a pressure line was connected to the tube on the high side, and a sampling tube was attached to the low side. Tests were made with the cell in a horizontal position.

Electrolyte solutions were made up from reagent grade KOH containing about 0.7 percent potassium carbonate (K_2CO_3). The concentration was determined as KOH by titration with standard acid to the phenolphthalein end point. At this end point (pH 8), carbonate is converted to bicarbonate so that values are slightly higher than the actual KOH content by about 0.2 percent. Three samples were collected while the cell was being drained to obtain an indication of any concentration gradient that might exist. Samples of about 3 grams were drained into vials assembled from capped stainless-steel tube fittings. The variation between samples never exceeded 0.3 percent with no consistent trend as to sequence. If any gradient developed during operation, it must have dissipated before the samples were taken.

Commercial reactant gases were used. Hydrogen (H_2) had a minimum purity level of 99.9 percent by volume and oxygen (O_2), 99.6 percent by volume. Flow rates of H_2 and O_2 were measured by float flowmeters. Hydrogen was vented continuously to maintain water balance in the cell by removing water evaporated into the gas cavity (ref. 4). When the rate was established, based on the assumption of equilibration of the gas with bulk electrolyte, the concentration was found to increase (i.e., excess water was re-

moved) while the cell was running. Since some oxygen was also vented to purge impurities, some water could have been removed thereby, although none was ever found in the room-temperature trap in the oxygen vent line, while an appreciable amount collected in the trap on the hydrogen side. A more likely explanation is that water tends to accumulate at the hydrogen electrode, where it is formed, thereby decreasing the electrolyte concentration and increasing the water vapor pressure. An empirical adjustment to 70 percent of the calculated vent rate eliminated this problem as far as could be determined.

A minimum oxygen vent rate was necessary at currents of 20 amperes (147 A/ft^2 or 1580 A/m^2) and higher. The excess amounted to the rate of consumption at a current of 12 amperes. With this rather substantial amount of venting, the voltage would level off to a steady value after 5 minutes of operation at a given current setting. Otherwise a further decline in voltage would be observed. No attempt was made to determine a level-off voltage as a function of vent rate. This procedure was accepted as an expedient to counteract the expected effect of pore blocking by the accumulation of impurities carried in with the oxygen (ref. 6).

Experimental Design

A number of considerations were involved with respect to selecting the experimental design grid for values of temperature and concentration:

(1) Since this study was exploratory, it was desirable to cover a considerable range for each variable. However, practical difficulties would be encountered at a low concentration and high temperature because of the high vapor pressure. For example, for 70 weight percent KOH at 460° F (511 K), the vapor pressure is 19 psia ($1.3 \times 10^5 \text{ N/m}^2$ abs), and, since the electrolyte was not confined, it would boil.

(2) There are also theoretical considerations regarding vapor pressure, which has a definite thermodynamic effect (appendix A) and would be expected to influence performance in general according to the principle of mass action.

(3) In the event of cell deterioration with time, obtaining at least the relative effects of temperature and concentration would be helpful.

(4) Only two runs could be made a day at two temperature levels and at a single concentration level.

In view of these considerations, the experimental design grid shown in figure 4 was selected. The centers of each block of four data points correspond to combinations of temperature and concentration producing approximately the same constant vapor pressure. The four data points in each group constitute a 2×2 factorial design that measures the direct incremental effects of temperature, concentration, and their interaction. The

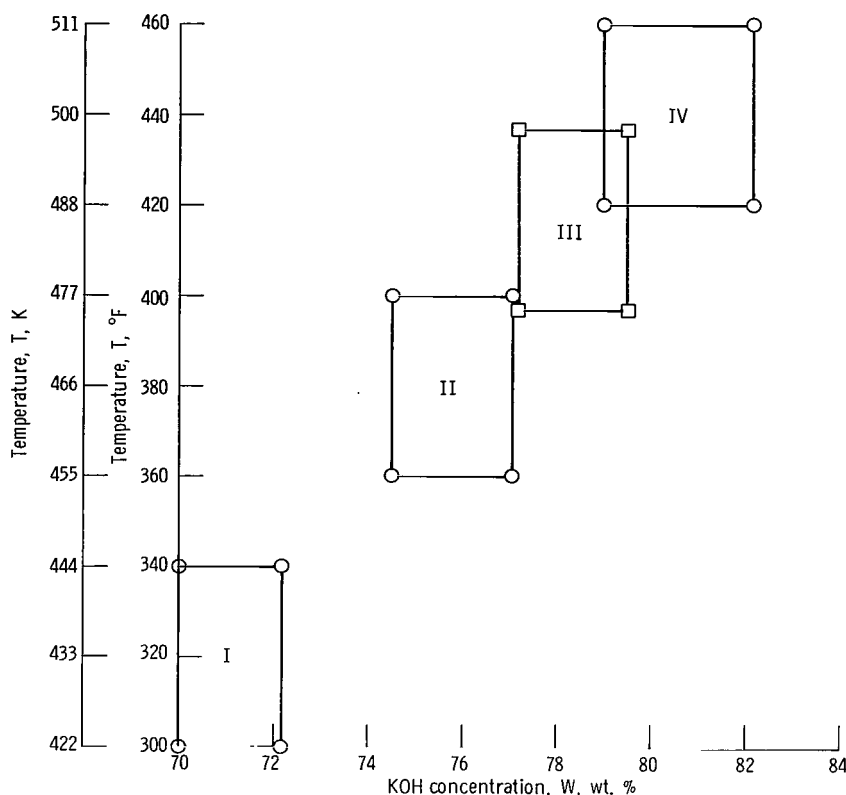


Figure 4. - Experimental design grid for values of temperature and concentration.

temperature range of each block was 40°F (22 K). Concentration ranges varied from 2.2 to 3.3 percent by weight.

Each block of experimental points is associated with a mean temperature, a mean concentration, and a mean level of cell performance. Since concurrent increases of temperature and concentration result in increased performance, the term performance level (denoted by Roman numerals) has been applied to designate the blocks.

RESULTS

The effects of concentration and temperature on cell performance at four performance levels, as defined in the Experimental Design section, are listed in table II as partial derivatives estimated by regression analysis (see appendix B for statistical analysis and table III for complete temperature-concentration raw data). These partial derivatives are the temperature and concentration coefficients in a linearized expression

for the variation of voltage with temperature and concentration at a given current density:

$$V - V_m = \left(\frac{\partial V}{\partial T} \right)_W (T - T_m) + \left(\frac{\partial V}{\partial W} \right)_T (W - W_m)$$

(All symbols are defined in appendix C.) The coefficients are presented graphically as functions of current density for the four performance level parameters in figures 5 and 6. Typical plots of voltage against current density are shown in figure 7. In this figure, a set of curves for one performance level is shown along with individual curves for the best and poorest performance obtained in the entire experiment.

The data in table II are presented as variations of voltage at current densities of

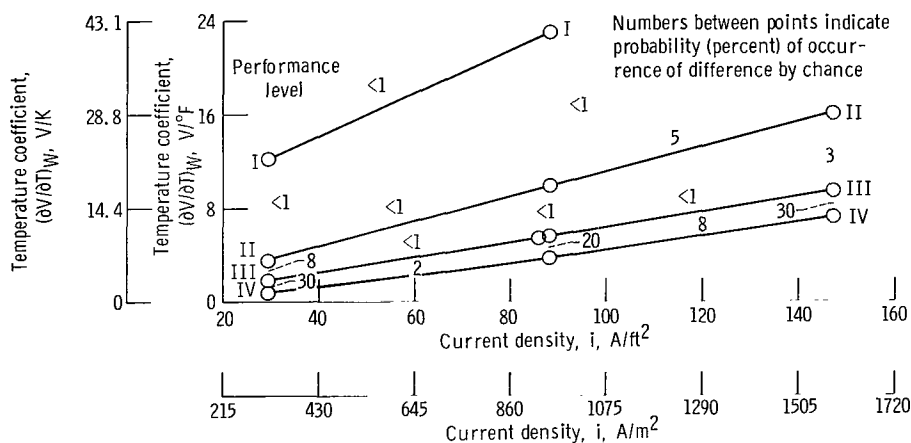


Figure 5. - Temperature coefficient as function of current density and parameters of performance level.

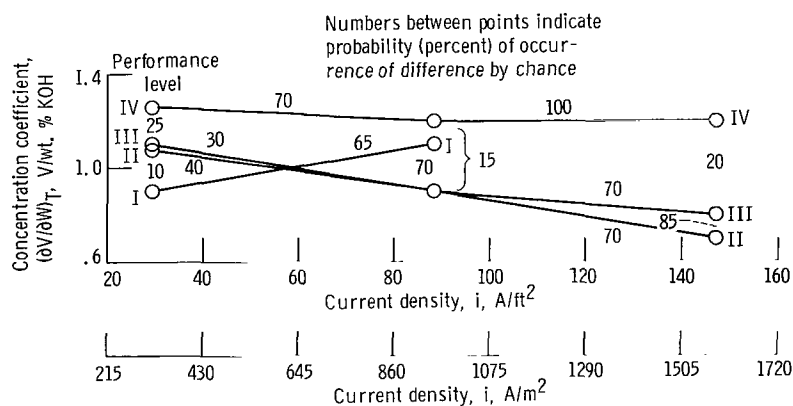


Figure 6. - Concentration coefficient as function of current density and parameters of performance level.

TABLE II. - EFFECT OF TEMPERATURE AND CONCENTRATION ON VOLTAGE AT CONSTANT CURRENT DENSITY

Performance level	Mean temperature in given performance level block, T_m		Mean concentration in given performance level block, W_m' wt. %	Current density, i		Mean value of voltage in given performance level block at given current density, V_m' V	Standard error of V_m' , s, V	Temperature coefficient of voltage at given current density, $(\partial V/\partial T)_W$		Standard error of $(\partial V/\partial T)_W$, s		Concentration coefficient of voltage, $(\partial V/\partial W)_T$, V/wt. % KOH	Standard error of $(\partial V/\partial W)_T$, s, V/wt. % KOH		Thermodynamic temperature coefficient of open-circuit voltage, $(\partial E_o/\partial T)_W$		Thermodynamic concentration coefficient of open-circuit voltage, $(\partial E_o/\partial W)_T$, V/wt. % KOH		Vapor pressure at mean temperature and mean concentration	
	$^{\circ}\text{F}$ K			A/ft^2 A/m^2				$^{\circ}\text{F}$ K		$^{\circ}\text{F}$ K			$^{\circ}\text{F}$ K		$^{\circ}\text{F}$ K		$^{\circ}\text{F}$ K		psia N/m^2 abs	
I	320	434	71.1	29.4	316	0.915	0.001	12.1 $\times 10^{-4}$	22 $\times 10^{-4}$	0.6 $\times 10^{-4}$	1 $\times 10^{-4}$	0.9 $\times 10^{-2}$	0.1 $\times 10^{-2}$	-5.2 $\times 10^{-4}$	-0.4 $\times 10^{-4}$	0.36 $\times 10^{-2}$		1.40	9 640	
				88.2	950	.737	.004	23 $\times 10^{-4}$	42 $\times 10^{-4}$	2	4	1.1	.4							
II	380	466	75.8	29.4	316	1.008	0.001	3.6 $\times 10^{-4}$	6.5 $\times 10^{-4}$	0.4 $\times 10^{-4}$	0.7 $\times 10^{-4}$	1.08 $\times 10^{-2}$	0.06 $\times 10^{-2}$	-5.5 $\times 10^{-4}$	-9.9 $\times 10^{-4}$	0.38 $\times 10^{-2}$		1.95	13 400	
				88.2	950	.889	.002	10	18	1	2	.9	.2							
				147	1580	.787	.005	16	30	2	4	.7	.4							
III	417	487	78.3	29.4	316	1.044	0.001	1.9 $\times 10^{-4}$	3.4 $\times 10^{-4}$	0.7 $\times 10^{-4}$	1.3 $\times 10^{-4}$	1.1 $\times 10^{-2}$	0.1 $\times 10^{-2}$	-5.1 $\times 10^{-4}$	-9.2 $\times 10^{-4}$	0.46 $\times 10^{-2}$		2.52	17 400	
				88.2	950	.943	.002	5.6	10.1	.8	1.4	.9	.14							
				147	1580	.859	.002	9.5	17	1.1	2	.8	.2							
IV	440	500	80.6	29.4	316	1.072	0.001	0.9 $\times 10^{-4}$	1.6 $\times 10^{-4}$	0.5 $\times 10^{-4}$	0.9 $\times 10^{-4}$	1.26 $\times 10^{-2}$	0.06 $\times 10^{-2}$	-5.0 $\times 10^{-4}$	-9.0 $\times 10^{-4}$	0.47 $\times 10^{-2}$		2.38	16 400	
				88.2	950	.974	.002	3.9	7.1	.8	1.4	1.2								
				147	1580	.894	.003	7.3	13.2	1.4	2.5	1.2								

29.4, 88.2, and 147 amperes per square foot (313, 950, and 1580 A/m², respectively). These points represent total currents of 4, 12, and 20 amperes through the test cells. The standard error values s are shown beneath the tabular entries. Based on the test for confidence limits (appendix B), the probability of exceeding $\pm 0.9 s$ by chance is 40 percent and for $\pm 1.9 s$ is 10 percent. The manner in which experimental error affects interpretation of the data is considered in appendix B. The probabilities for chance occurrence of differences in values of the coefficients are indicated between corresponding points in figures 5 and 6.

An interpretation of these results, which were obtained without the benefit of a reference electrode, would be ambiguous if it were not for other published work on cells of this type by Bacon (ref. 2, p. 144) and by Rockett and Brown (refs. 5 and 7). These investigators found that at the current densities employed in this work, the oxygen electrode is responsible for more than half the overall polarization and for all the fixed loss and nonlinear character. Since the reversibility of hydrogen electrodes and the irreversibility of oxygen electrodes is well recognized (ref. 8, pp. 544 and 615), it was assumed for the present investigation that the observed effects are largely attributable to the oxygen electrode, at least for current densities of 88.2 amperes per square foot (950 A/m²) or less.

One manifestation of the irreversibility of the oxygen electrode that became apparent in the course of this investigation was a marked time dependence of the open-circuit voltage. For example, it was observed that when the current was increased or decreased to a nonzero value, a stable voltage (to within ± 1 mV) was obtained within 5 minutes. On the other hand, at the highest temperature studied (460° F or 511 K), a stable open-circuit voltage was not obtained for at least 10 minutes. while at 300° F (422 K), the open-circuit voltage continued to rise slowly after 6 hours. That the effect is peculiar to the oxygen electrode is confirmed by similar behavior observed in the attainment of open-circuit voltage when oxygen was applied to the electrode at startup. (Hydrogen electrode response was stabilized at all temperatures within 5 min.)

In lieu of stabilized open-circuit voltages, the voltages recorded 1 minute after opening the circuit are listed in table III as $V_O^{1 \text{ min}}$. The estimated polarization based on E_O , the theoretical value (appendix A), is listed as

$$\eta_O^{1 \text{ min}} = E_O - V_O^{1 \text{ min}}$$

These data permit some estimate to be made of IR-free losses.

The variability of the results, as shown by the magnitude of the standard error s , may also be attributed to the oxygen electrode in view of the sensitivity of cell performance to interface location (discussed in connection with experimental procedure). Dislocations and redistributions may be induced by filling and emptying the cell, changes

TABLE III. - TEMPERATURE-CONCENTRATION DATA (RAW)

Run	Temperature, T		Concentration, W, wt. %	Voltage at current density i , V_i , V			Voltage 1 minute after circuit is opened, $V_o^{1 \text{ min}}$, V	Open-circuit voltage calculated according to thermo- dynamic principle, E_o , V	Polarization 1 minute after circuit is opened, $\eta_o^{1 \text{ min}}$, V
	°F	K		Current density, i , A/ft ² (A/m ²)					
				29.4(316)	88.2(950)	147(1580)			
57	300	422	69.7	0.882	0.688	-----	1.063	1.212	0.149
53	↓	↓	70.2	.880	.664	-----	1.068	1.214	.146
58	↓	↓	72.1	.902	.702	-----	1.080	1.221	.141
52	↓	↓	72.3	.898	.708	-----	1.080	1.221	.141
56	340	444	69.7	0.928	0.778	-----	1.072	1.191	0.119
54	↓	↓	70.2	.928	.763	-----	1.075	1.193	.118
59	↓	↓	72.1	.950	.797	-----	1.093	1.200	.107
51	↓	↓	72.3	.950	.798	-----	1.095	1.201	.106
22	360	455	74.5	0.988	0.854	0.734	1.115	1.200	0.085
15	↓	↓	74.6	.990	.865	.759	1.115	1.200	.085
17	↓	↓	77.1	1.013	.884	.774	1.133	1.210	.077
20	↓	↓	77.1	1.014	.874	.748	1.136	1.210	.074
21	400	477	74.5	0.999	0.894	0.804	1.118	1.178	0.060
16	↓	↓	74.6	1.002	.900	.814	1.121	1.178	.057
18	↓	↓	77.1	1.032	.926	.841	1.144	1.188	.044
19	↓	↓	77.1	1.030	.917	.820	1.144	1.188	.044
11	397	476	77.1	1.030	0.924	0.834	1.140	1.191	0.051
39	↓	↓	77.3	1.028	.920	.832	1.140	1.191	.051
38	↓	↓	79.4	1.050	.939	.843	-----	1.200	-----
13	↓	↓	79.5	1.054	.943	.853	1.160	1.200	.040
12	437	498	77.1	1.038	0.945	0.870	1.141	1.169	0.028
40	↓	↓	77.3	1.032	.940	.866	1.138	1.169	.031
37	↓	↓	79.4	1.057	.960	.881	1.158	1.181	.023
14	↓	↓	79.5	1.065	.971	.897	1.163	1.181	.018
23	420	488	78.9	1.050	0.944	0.854	1.158	1.187	0.029
30	↓	↓	79.0	1.053	.953	.870	1.160	1.187	.027
28	↓	↓	82.1	1.090	.985	.900	1.186	1.201	.015
25	↓	↓	82.4	1.090	.982	.892	1.187	1.201	.014
24	460	511	78.9	1.054	0.958	0.879	1.150	1.166	0.016
29	↓	↓	79.0	1.050	.961	.891	1.148	1.166	.018
27	↓	↓	82.1	1.093	1.002	.932	1.173	1.182	.009
26	↓	↓	82.4	1.100	1.006	.931	1.174	1.183	.009

in temperature and concentration, and evaporation of water during the period of overnight stand. This suggestion of an adjustment process is reinforced by experience with freshly prepared cells, which usually perform relatively poorly at first. The effects of incomplete wetting or of interface dislocation would be manifested as changes in the effective area or the internal resistance, and therefore, the magnitude of the interface effect would vary with current. The standard errors shown in table II conform to this reasoning.

DISCUSSION

Because of the scatter in the data, rigorous conclusions cannot be drawn regarding the effects of temperature and concentration on cell performance. However, certain qualitative trends merit consideration. In assessing the significance of these trends, a rather liberal test of 20 percent probability of chance occurrence was applied.

In brief, the temperature coefficient $(\partial V/\partial T)_W$ decreases with increasing performance level and increases with increasing current. The behavior of the concentration coefficient $(\partial V/\partial W)_T$ is not consistent, and differences with respect to performance level and current are attended with high probabilities of chance occurrence. (See figs. 5 and 6.) As a whole, values of the concentration coefficient are about double the values calculated from theory $(\partial E_o/\partial W)_T$ (appendix A) based on the effect of concentration on water vapor pressure (see table II).

Some variation of the coefficients with current can be expected to result from the effects of temperature and concentration on electrolyte conductivity. Qualitatively, this variation is apparent in figure 7, where vertical differences between appropriate curves are proportional to the coefficients. Thus, for example, in figure 7, curves 16 and 18 measure the concentration coefficient $(\partial V/\partial W)_T$ at 400° F and curves 17 and 18 measure the temperature coefficient $(\partial V/\partial T)_W$ at 77.1 weight percent KOH. The divergence of curves 17 and 18 with increasing current is obvious. This is expected because the curve for higher temperature (18) lies generally above the one for lower temperature (17) and has a smaller slope because of a greater electrolyte conductivity at the higher temperature. On the other hand, when curves 16 and 18 are inspected closely, they are seen to converge. In this case, the curve for higher concentration (18) lies generally above that for the lower concentration (16) but has a larger slope because of a lower electrolyte conductivity at the higher concentration.

Inasmuch as these qualitative considerations of the conductivity effect have a bearing on interpretation of the data, a quantitative estimate of the expected variation of the coefficients with current is in order. The following derivation provides expressions that can be used with data from table II and conductivity data from reference 3 to

make a convenient comparison of estimated and observed current density effects on the coefficients.

Two linear polarization curves designated 1 and 2 are considered. These curves correspond to temperatures T_1 and T_2 or to concentrations W_1 and W_2 . For these curves, effects from sources other than conductivity are assumed not to vary with current. For the temperature relations, by definition,

$$\left(\frac{\partial V}{\partial T}\right)_{W,i} = \frac{V_2 - V_1}{T_2 - T_1} \quad (1)$$

The estimate desired is

$$\frac{\Delta \left(\frac{V_2 - V_1}{T_2 - T_1} \right)}{\Delta i} = \frac{1}{T_2 - T_1} \left(\frac{\Delta V_2}{\Delta i} - \frac{\Delta V_1}{\Delta i} \right) = \left(\frac{1}{T_2 - T_1} \right) \left(\frac{1}{\Delta i} \right) (\Delta V_2 - \Delta V_1) \quad (2)$$

Since

$$\frac{\Delta V}{\Delta i} \propto \frac{1}{K} \quad (3)$$

where K is the conductivity,

$$\frac{\Delta V_2}{\Delta V_1} = \frac{K_1}{K_2}$$

Thus, by subtraction of 1 from both sides,

$$\frac{\Delta V_2 - \Delta V_1}{\Delta V_1} = \frac{K_1 - K_2}{K_2} \quad (4a)$$

and by addition of 1 to both sides,

$$\frac{\Delta V_2 + \Delta V_1}{\Delta V_1} = \frac{K_1 + K_2}{K_2} \quad (4b)$$

Substituting equation (4a) in equation (2) after transposing ΔV_1 to the right side yields

$$\frac{\Delta \left(\frac{V_2 - V_1}{T_2 - T_1} \right)}{\Delta i} = \frac{1}{\Delta i} \left(\frac{K_1 - K_2}{T_2 - T_1} \right) \frac{\Delta V_1}{K_2} \quad (5)$$

The term $\Delta V_1/K_2$ can be replaced by a form containing mean values ΔV_m and K_m .
Since

$$\left. \begin{aligned} \frac{\Delta V_2 + \Delta V_1}{2} &= \Delta V_m \\ \frac{K_1 + K_2}{2} &= K_m \end{aligned} \right\} \quad (6)$$

and from equation (4b),

$$\frac{\Delta V_2 + \Delta V_1}{K_1 + K_2} = \frac{\Delta V_1}{K_2} \quad (7)$$

$$\frac{\Delta V_1}{K_2} = \frac{\Delta V_m}{K_m} \quad (8)$$

Note that the mean values of K and ΔV for the two temperatures at the mean concentration become the mean values of K and ΔV for the block. Therefore,

$$\frac{\Delta \left(\frac{V_2 - V_1}{T_2 - T_1} \right)}{\Delta i} = \frac{1}{\Delta i} \left(\frac{-\Delta K}{\Delta T} \right) \frac{\Delta V_m}{K_m} \quad (9)$$

Similarly, for the concentration coefficient,

$$\frac{\Delta \left(\frac{V_2 - V_1}{W_2 - W_1} \right)}{\Delta i} = \frac{1}{\Delta i} \left(\frac{-\Delta K}{\Delta W} \right) \frac{\Delta V_m}{K_m} \quad (10)$$

where K_m and V_m , the mean values of K and ΔV for the block, are the same in both the expression for temperature and for concentration.

These expressions can be used in conjunction with the data of table II and the conductivity data of reference 3 to compare estimated and observed effects of current density on the coefficients. For a given performance level and two specified values of current density i , values of V_m can be found and used to determine ΔV_m . From conductivity data at the mean condition (T_m , W_m), K_m can be determined. Similarly, $\Delta K/\Delta T$ or $\Delta K/\Delta W$ can be determined over a range of T or W including the mean condition. For purposes of comparison, the denominator Δi can be eliminated. This procedure was carried out, and the results are listed in table IV.

The observed effect of current density is greater than that predicted for the temperature coefficient and less than that predicted for the concentration coefficient. However, although the observed effect of current density on the temperature coefficient is significant (less than 10 percent probability of chance occurrence), the significance of current-density-related differences in the concentration coefficient is highly doubtful (greater than 30 percent probability of chance occurrence) (figs. 5 and 6). The principal reason for the loss of significance in this case is that the differences in question are relatively small. Thus, while the concentration coefficients are generally significant (at a 20-percent level of chance occurrence), their variation is not, and the suggestion of current independence is not refuted. On the other hand, neither is the possible existence of a real conductivity effect refuted.

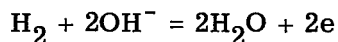
The appearance of compensation for a conductivity effect in the case of the concentration coefficient and for enhancement in the case of the temperature coefficient is consistent with known and theoretically predictable behavior of the hydrogen electrode. In their paper on the hydrogen electrode, Rockett and Brown (ref. 7) included polarization curves for the hydrogen electrode against a reference electrode at various temperature parameters. The relative slopes of these nearly linear curves are consistently greater than the ratios of corresponding reciprocal conductivities, thus indicating an effect of temperature that is supplementary to the conductivity effect. Rockett and Brown's paper did not include concentration parameters that would furnish information comparable to that relating to temperature. However, other effects related to concentration should operate in a direction opposed to the conductivity effect because the half-cell reaction

TABLE IV. - CALCULATED AND OBSERVED EFFECTS OF ELECTROLYTE CONDUCTIVITY ON VARIATION OF TEMPERATURE
AND CONCENTRATION COEFFICIENTS OF VOLTAGE WITH CURRENT DENSITY^a

Performance level	Variation in mean voltage in given performance level block between given current densities, ^a ΔV_m , V	Mean value of conductivity for performance level block, K_m , (ohm-cm) ⁻¹	Temperature coefficient of conductivity, $\Delta K/\Delta T$, [ohm-cm(K)] ⁻¹	Calculated effect of current density on temperature coefficient of voltage, $\Delta(V_2 - V_1/T_2 - T_1)$		Observed variation in temperature coefficient of voltage, $\Delta(\partial V/\partial T)_W$		Concentration coefficient of conductivity, $\Delta K/\Delta W$, [(ohm-cm)(wt. %)] ⁻¹	Calculated effect of current density on concentration coefficient, $\Delta(V_2 - V_1/W_2 - W_1)$, V/wt. %	Observed variation in concentration coefficient of voltage, $\Delta(\partial V/\partial W)_T$, V/wt. %
				$V/^{\circ}\text{F}$	V/K	$V/^{\circ}\text{F}$	V/K			
I	-0.178	1.66	0.012	7×10^{-4}	13×10^{-4}	11×10^{-4}	21×10^{-4}	-0.038	-0.4×10^{-2}	$+0.2 \times 10^{-2}$
II	-.102	1.84	.014	4	8	6.5	12	-.045	-.3	-.15
III	-.084	2.03	.013	3	5	4	7	-.052	-.2	-.1
IV	-.080	2.05	.013	3	5	3.4	6	-.052	-.2	0

^aValues of current density for performance level I, 29.4 and 88.2 A/ft² (316 and 950 A/m²); for performance levels II to IV, 88.2 and 147 A/ft² (950 and 1580 A/m²).

suggests that both mass action and transport benefits are derived from increased hydroxyl ion activity and decreased water activity:



(Mass action effects, of course, require that reaction orders be nonzero with respect to the reactants.)

An increase in performance from an increase in temperature is not surprising because of the relation of temperature to rate processes in general. However, for the reaction $\text{H}_2 + 1/2 \text{O}_2 = \text{H}_2\text{O}$, the thermodynamic temperature coefficient of voltage $(\partial E_{\text{O}}/\partial T)_{\text{W}}$ is negative and is in fact of the same order of magnitude as the observed coefficients $(\partial V/\partial T)_{\text{W}}$ (table II). Conceivably, polarization curves for two different temperatures could cross with the curve for the higher temperature starting lower but falling less rapidly than that for the lower temperature. However, the voltages observed 1 minute after opening the circuit $V_{\text{O}}^1 \text{ min}$ (table III) indicate that an appreciable temperature-dependent fixed loss exists in the system so that even at open circuit, the actual temperature coefficient is positive. A similar effect was reported by Bacon (ref. 3, p. 149).

With an increase in performance level, a closer approach to equilibrium open-circuit conditions is attained, as shown by the values of $\eta_{\text{O}}^1 \text{ min}$ (table III). It follows that the temperature coefficient should decrease with an increase in performance level, since all kinetic contributions must converge to zero at the equilibrium condition.

From inspection of figure 7, the current-independent aspect of the effect of increased concentration can be seen as a general upward shifting of the polarization curve. Table II shows that the magnitude of this shift at all performance levels is two or more times that attributable to the depression of water vapor pressure (i.e., $(\partial E_{\text{O}}/\partial W)_{\text{T}}$), except for some cases at the highest current level where the conductivity effect is important. A comparison of the concentration coefficient for the conditions of Bacon's work can be obtained from figure 1, where at 50 amperes per square foot (540 A/m^2) an increase of 0.1 volt for an 8 percent concentration change is found. The resulting value of 1.25×10^{-2} volt per percent for $(\partial V/\partial W)_{\text{T}}$ is consistent with the results of this work.

Unlike the temperature coefficient, the concentration coefficient does not show a tendency to decrease with increasing performance level as would be expected for a kinetic mechanism as equilibrium is approached. Actually, in most cases the concentration coefficient increases with performance level (fig. 6), although the differences have at best only borderline significance. If the scheme of the experimental design is followed, voltages in excess of theoretical would be indicated at still higher performance levels than those investigated, since the concentration coefficient tends to be at

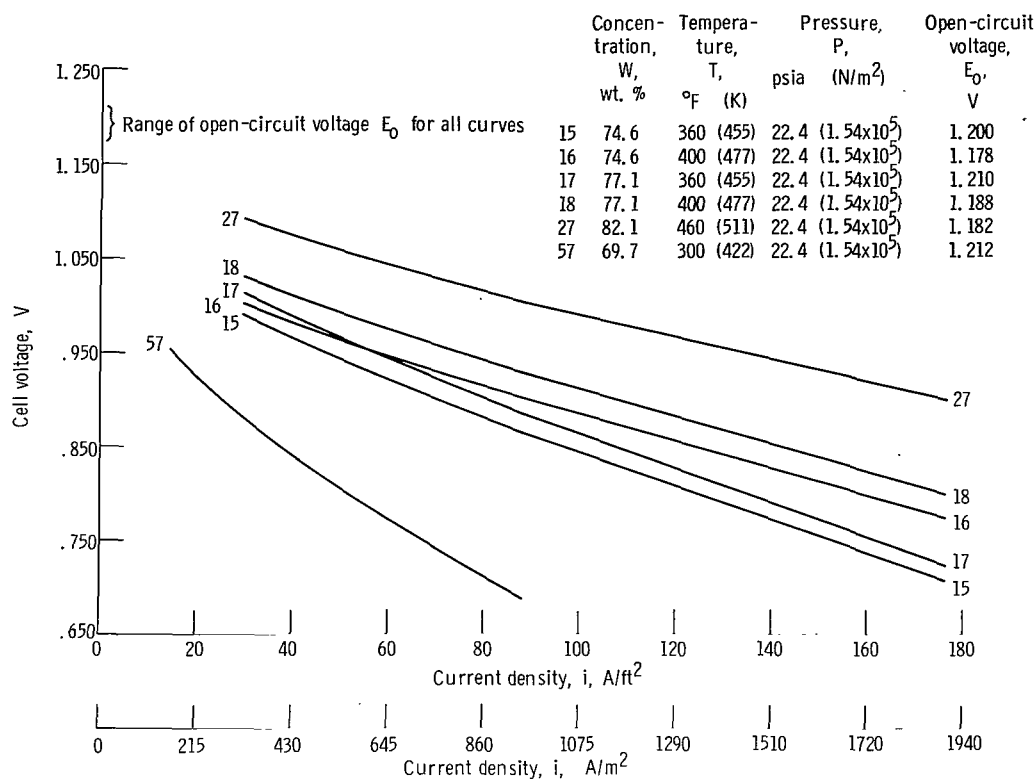


Figure 7. - Effect of temperature and concentration on performance.

least twice the theoretical rate of increase of open-circuit voltage with concentration. Clearly, if a conflict with the laws of thermodynamics is to be avoided, the concentration coefficient must ultimately decrease with increasing performance level. However, the voltage data from which the coefficients were estimated have values less than the theoretical open-circuit voltage by at least 80 millivolts, so that there is an ample reserve of polarization to be overcome.

The uniformity of the effect of concentration with respect to current and performance level lends weight to the hypothesis that current-related effects from reaction kinetics, mass transport, and internal resistance are superimposed on an open-circuit value established by the magnitude of the characteristic fixed loss found at the oxygen electrode and that the effect of concentration is manifested as a variation in this fixed loss.

The time dependence of the open-circuit voltage raises the question of just what mechanism the fixed loss is related to. There may be parallel reaction paths, one of which is so highly polarized that it contributes a negligible amount of the total current but has little or no fixed loss. The other path, which contributes substantially all the current, is then associated with the fixed loss and has polarization characteristics typically related to temperature and the catalytic activity of the reaction surface. With

respect to this activity, it is of interest to note that platinum-catalyzed electrodes show no such time dependence of the open-circuit voltage as was encountered herein with the porous nickel electrodes. Other work done in this laboratory (unpublished data obtained by N. Hagedorn of Lewis) on cells operating at 150° F (339 K) in a solution of 35 percent by weight KOH revealed that, with platinum-catalyzed electrodes, stable open-circuit voltages were attained in less than 1 minute. These open-circuit voltages are substantially below theoretical with fixed losses of about 100 millivolts.

The behavior of both temperature and concentration coefficients with a variation in current density and the behavior of the temperature coefficient with a variation in the performance level parameter can be related qualitatively to mass action effects, conductance variations, and kinetic principles. The seemingly anomalous behavior of the concentration coefficient with respect to the performance level parameter invites further exploration of the mechanism of the oxygen electrode in KOH concentrations above 35 percent by weight.

CONCLUDING REMARKS

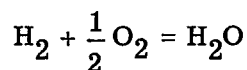
From the results of the experimental work reported herein, the effect of temperature appears to be a typical rate-process phenomenon, whereas the effect of concentration appears to be associated with an unresolved mechanism that is responsible for the fixed (current-independent) loss at the oxygen electrode.

Lewis Research Center,
National Aeronautics and Space Administration,
Cleveland, Ohio, December 26, 1968,
120-34-02-24-22.

APPENDIX A

THEORETICAL VOLTAGES FOR HYDROGEN-OXYGEN-WATER SYSTEM ESTIMATED FROM THERMODYNAMIC DATA

For the reaction



at the standard state (hypothetical) of unit fugacity and enthalpy of the real gas at zero pressure and a temperature of 25° C (298 K), the following thermodynamic values apply (ref. 9, p. 1576):

TABLE V. - THERMAL PROPERTIES OF HYDROGEN,
OXYGEN, AND WATER AT THE STANDARD STATE

Substance	Enthalpy of formation, ΔH_f^0 , kcal/(g)(mole)	Entropy, S^0 , cal/(g)(mole)(K)	Free energy of formation, ΔG_f^0 , kcal/(g)(mole)
Hydrogen	0	31.21	0
Oxygen	0	49.00	0
Water	-57.80	45.11	-54.64

The electromotive force of a reversible cell for which the net reaction applies is

$$E_o = -\frac{\Delta G}{nF}$$

For this reaction as written, $n = 2$.

The variation of E_o with fugacity (with pressure for gases behaving ideally) is

$$\Delta E_o = \frac{RT}{nF} \ln \frac{f_{\text{H}_2} f_{\text{O}_2}^{1/2}}{f_{\text{H}_2\text{O}}}$$

where the difference is referred to the standard state.

The best available reference data on the thermodynamic properties of H_2 , O_2 , and H_2O (refs. 10 and 11) were used to study the behavior of the hydrogen-oxygen-water system. These data were particularly useful for the purpose of determining whether or not nonideality of the gases under real conditions of temperature and pressure is enough to cause errors of 1 millivolt in the estimation of E_o when fugacity is assumed equal to partial pressure. (Corrections for nonideality due to mixing were not accounted for.) Up to $620^\circ F$ (600 K) and 600 psi ($41 \times 10^5 \text{ N/m}^2$), the nonidealities of H_2 and O_2 together contribute less than the equivalent of ± 0.5 millivolt error. For H_2O under Bacon's condition, where the vapor pressure was about 150 psia ($10 \times 10^5 \text{ N/m}^2$) and the temperature was $392^\circ F$ (473 K), an error of 1 millivolt is contributed by nonideality. However, at all conditions of this work, the error in the estimation of E_o was negligible.

Corrections for pressure can therefore be made according to the following formula (where ΔE_o is in mV, constants are lumped, and pressure in atmospheres is substituted for fugacity):

$$\Delta E_o = 0.0992 \text{ T(K)} \log \frac{P_{H_2} P_{O_2}^{1/2}}{P_{H_2O}}$$

$$= 0.0551 \text{ T}(^{\circ}\text{R}) \log \frac{P_{H_2} P_{O_2}^{1/2}}{P_{H_2O}}$$

$$= 0.0431 \text{ T(K)} \ln \frac{P_{H_2} P_{O_2}^{1/2}}{P_{H_2O}}$$

$$= 0.02394 \text{ T}(^{\circ}\text{R}) \ln \frac{P_{H_2} P_{O_2}^{1/2}}{P_{H_2O}}$$

The water vapor pressure over KOH solutions was estimated from the data of reference 12 (and private communication with Pratt & Whitney Aircraft).

The relation of standard-state reversible electromotive force to temperature over the normal operating range of aqueous fuel cells is nearly linear so that it may be represented by two straight lines, as shown in figure 8.

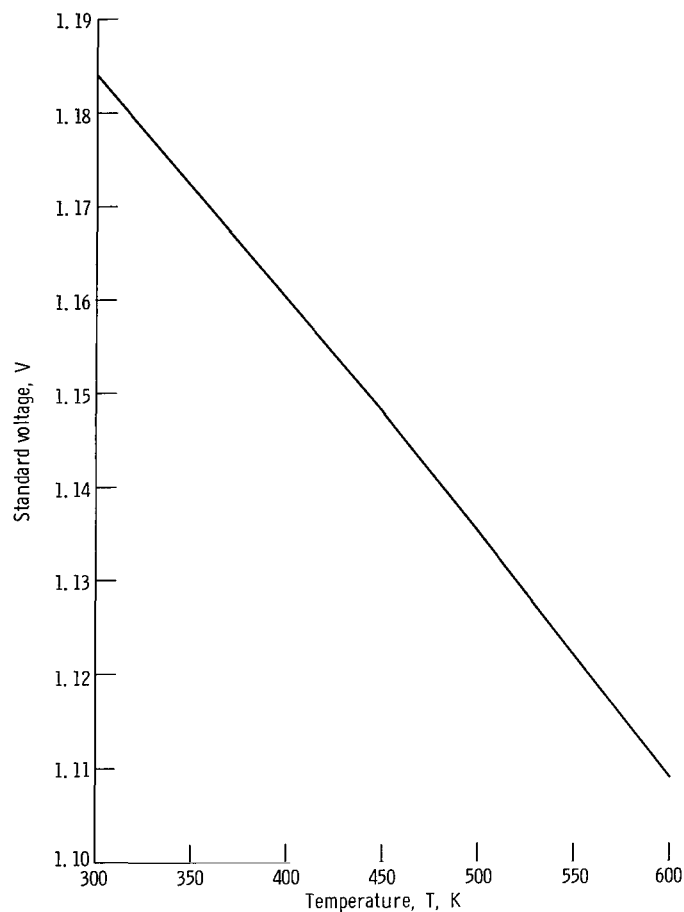


Figure 8. - Standard-state voltage for reaction $\text{H}_2 + \frac{1}{2} \text{O}_2 = \text{H}_2\text{O}$.

APPENDIX B

STATISTICAL ANALYSIS OF DATA

Data were obtained to determine the effects of concentration and temperature on cell performance at four performance levels. The resulting temperature and concentration coefficients are presented in table II as partial derivatives estimated by regression analysis. These data were treated according to methods outlined by Davies (ref. 13, chs. 3, 4, 7, and 8) and were fitted to the following linearized expression for the variation of voltage with temperature and concentration at a given current density:

$$V - V_m = \left(\frac{\partial V}{\partial T} \right)_W (T - T_m) + \left(\frac{\partial V}{\partial W} \right)_T (W - W_m)$$

(The coefficient for a term in $(T - T_m)(W - W_m)$ was also estimated but was not found to be significant.) The residual standard error s was estimated from the data. This quantity measures the variability not accounted for by the direct effects of T and W . From s , the standard errors of the coefficients are obtained, and the probability of a given value occurring by chance is estimated from the t -test (Student's t) for confidence limits (see table II for probabilities).

For the analysis, the calculations were simplified because the performance level blocks (fig. 4) were semiorthogonal (only two values of T but distributed values of W). Let

$$T - T_m = x$$

$$W - W_m = y$$

$$V - V_m = z$$

and

$$\left(\frac{\partial V}{\partial T} \right)_W = a$$

$$\left(\frac{\partial V}{\partial W} \right)_T = b$$

Then

$$a = \frac{\sum xz}{\sum x^2} \quad b = \frac{\sum yz}{\sum y^2}$$

and

$$s = \left(\frac{\sum z^2 - a \sum xz - b \sum yz}{5} \right)^{1/2}$$

where 5 is the number of degrees of freedom, which, in this case, is the total number of data points (8) minus the number of quantities estimated (3), that is, V_m , a , and b . The standard error of a coefficient is estimated from

$$s(a) = \left(\frac{s}{\sum x^2} \right)^{1/2}$$

The t-test for confidence limits is concerned with the distribution of a quantity t that is a function of a probability α and the number of degrees of freedom of an estimated quantity. The probability α that the true value of the quantity differs from the estimated value by as much as (t) (s) is the basis for determining the precision of the data. The probability that the true value of a , for example, lies between $a + ts$ and $a - ts$ is $(1 - 2\alpha)$.

The standard error shown for the mean voltage V_m (table II) indicates the variability of the mean of eight tests. The variability from test to test would be greater than that of the mean of eight tests by a factor of $\sqrt{8}$ (about 3).

Probabilities for the chance occurrence of the observed difference in any two coefficients are determined in a less straightforward manner than those for the occurrence of differences in the true and estimated quantities (ref. 13, p. 164) because the degrees of freedom need to be adjusted for differences in standard errors. Differences in coefficients to be tested for significance are those within performance levels for the effect of current and those between performance levels at the same current.

The probabilities of chance occurrence for the variations with current within performance levels for the concentration coefficients $(\partial V / \partial W)_T$ are fairly high, greater than 30 percent in all cases (fig. 6). On the other hand, the probabilities of chance occurrence for variations with current for the temperature coefficients $(\partial V / \partial T)_W$ within performance levels are 8 percent or less.

APPENDIX C

SYMBOLS

a	$(\partial V / \partial T)_W$
b	$(\partial V / \partial W)_T$
E_o	open-circuit voltage calculated according to thermodynamic principles, V
F	Faraday constant, 96 493 C/g-equivalent
f	fugacity, atmos; N/m^2
ΔG_f^o	free energy of formation, kcal/g-mole
ΔH_f^o	enthalpy of formation, kcal/g-mole
i	current density, A/ft^2 ; A/m^2
K	electrolytic conductivity, $(ohm-cm)^{-1}$
K_m	mean value of K for performance level block, $(ohm-cm)^{-1}$
n	number of electrons involved in given electrochemical reaction
P	pressure, atmos; N/m^2
R	gas constant, 8.314 J/(mole)(K)
S	entropy, cal/(g-mole)(K)
s	standard error in units of quantity for which it is estimated
T	temperature, $^{\circ}F$; K
T_m	mean value of T in given performance level block, $^{\circ}F$; K
t	Student's t, dimensionless
V	voltage, V
V_i	value of V at current density i, V
V_m	mean value of V in given performance level block at given current density, V
$V_o^{1 \text{ min}}$	value of V obtained 1 minute after circuit is opened, V
W	electrolyte concentration, wt. %
W_m	mean value of W in given performance level block, wt. %
x	$T - T_m$

y $W - W_m$

z $V - V_m$

α probability of occurrence of difference by chance

$\eta_o^{1 \text{ min}}$ polarization 1 minute after circuit is opened $\eta_o^{1 \text{ min}} = E_o - V_o^{1 \text{ min}}$

REFERENCES

1. Young, G. J., ed.: Fuel Cells. Reinhold Publ. Corp., 1960.
2. Vogel, W. M.; Routsis, K. J.; Kehrer, V. J.; Landsman, D. A.; and Tschinkel, J. G.: Some Physicochemical Properties of the KOH-H₂O System. Range: 55 to 85 Weight % and 120⁰ to 250⁰ C. J. Chem. Eng. Data, vol. 12, no. 4, Oct. 1967, pp. 465-472.
3. Mitchell, Will, Jr., ed.: Fuel Cells. Academic Press, 1963.
4. Latimer, Howard J., Jr.; Ching, Albert C.; Greenwood, Calvin D.; and Dixon, Robert W.: Design and Development of Hydrogen-Oxygen Fuel Cell Powerplant. Rep. PWA-2081, Pratt & Whitney Aircraft (NASA CR-51544), June 15, 1962.
5. Rockett, John A.; and Brown, Ralph: Theory of the Performance of Porous Fuel Cell Electrodes. J. Electrochem. Soc., vol. 113, no. 3, Mar. 1966, pp. 207-213.
6. Swinkles, D. A. J.: Impurity Effects in High Current Density Cl₂ Electrodes. J. Electrochem. Soc., vol. 114, no. 8, Aug. 1967, pp. 812-816.
7. Brown, Ralph; and Rockett, John A.: The Performance of Flooded Porous Fuel Cell Electrodes. J. Electrochem. Soc., vol. 113, no. 9, Sept. 1966, pp. 865-870.
8. Vetter, Klaus, J. (Scripta Technica, trans.): Electrochemical Kinetics. Academic Press, 1967.
9. Lange, N. A.; and Forker, G. M., eds.: Handbook of Chemistry. Tenth ed., McGraw-Hill Book Co., Inc., 1961.
10. Hilsenrath, Joseph; Beckett, Charles W.; Benedict, William S.; Fano, Lilla; Hoge, Harold J.; Masi, Joseph F.; Nuttall, Ralph L.; Touloukian, Yerman S.; and Woolley, Harold W.: Tables of Thermal Properties of Gases. Circ. No. 564, National Bur. Standards, Nov. 1, 1955.
11. Keenan, Joseph H.; and Keyes, Frederick G.: Thermodynamic Properties of Steam. John Wiley & Sons, Inc., 1936.
12. Clifford, John; and Faust, Charles: Research on the Electrolysis of Water with a Hydrogen-Diffusion Cathode to be used in a Rotating Cell. Battelle Memorial Inst. (AMRL-TDR-62 94), Aug. 1962. AF33 (616)-8431.
13. Davies, Owen L., ed.: Statistical Methods in Research and Production. Third ed., Hafner Publ. Co., Inc., 1957.

FIRST CLASS MAIL

020 001 28 51 3DS 69086 00903
AIR FORCE WEAPONS LABORATORY/AFWL/
KIRTLAND AIR FORCE BASE, NEW MEXICO 87111

ATTN: LOU BOWMAN, ACTING CHIEF TECH. LI.

POSTMASTER: If Undeliverable (Section 158
Postal Manual) Do Not Return

"The aeronautical and space activities of the United States shall be conducted so as to contribute . . . to the expansion of human knowledge of phenomena in the atmosphere and space. The Administration shall provide for the widest practicable and appropriate dissemination of information concerning its activities and the results thereof."

— NATIONAL AERONAUTICS AND SPACE ACT OF 1958

NASA SCIENTIFIC AND TECHNICAL PUBLICATIONS

TECHNICAL REPORTS: Scientific and technical information considered important, complete, and a lasting contribution to existing knowledge.

TECHNICAL NOTES: Information less broad in scope but nevertheless of importance as a contribution to existing knowledge.

TECHNICAL MEMORANDUMS: Information receiving limited distribution because of preliminary data, security classification, or other reasons.

CONTRACTOR REPORTS: Scientific and technical information generated under a NASA contract or grant and considered an important contribution to existing knowledge.

TECHNICAL TRANSLATIONS: Information published in a foreign language considered to merit NASA distribution in English.

SPECIAL PUBLICATIONS: Information derived from or of value to NASA activities. Publications include conference proceedings, monographs, data compilations, handbooks, sourcebooks, and special bibliographies.

TECHNOLOGY UTILIZATION PUBLICATIONS: Information on technology used by NASA that may be of particular interest in commercial and other non-aerospace applications. Publications include Tech Briefs, Technology Utilization Reports and Notes, and Technology Surveys.

Details on the availability of these publications may be obtained from:

SCIENTIFIC AND TECHNICAL INFORMATION DIVISION
NATIONAL AERONAUTICS AND SPACE ADMINISTRATION
Washington, D.C. 20546